Coordinated Framework for Voltage Control in Distribution System with Wind Energy

Joseph O. Petinrin, Oluyemi O. Petinrin, Moses O. Petinrin, and Ikeoluwa I. Ogedengbe

Abstract— **The developed hierarchical framework for voltage control in distribution system with high penetration of wind generation presented in this paper does not only consider how voltage/VAr control (VVC) devices are coordinated, but it also provides an equitable dispatch by managing energy storage systems and demand response options in a chronological timescale. In contrast to current methods in the literature, which typically optimize the size and sitting of wind generating for negligible grid impacts, the incumbent paper adopts a plug-and-play approach for wind integration, where system operators dispatch existing VVC devices and non-generation resources to handle the system in its current situation and maintain the voltage profile. The latter modelling approach conforms to the latest modus operandi of the dense connection of wind generation to achieve the net zero vision. In order to reduce voltage variations and energy losses, the issue is framed as a significant nonlinear optimization problem. A Hybrid Particle Swarm Optimization/Gravitational Search Algorithm (PSOGSA) is used to determine the optimal size and location of the energy storage and optimal customer's electricity consumption scheduling to protect the system voltage profile from wind energy's erratic qualities The efficiency of the developed technique is verified using a quasi-static time series analysis conducted during a 24-hour simulation period on an IEEE 123 node test feeder using MATLAB com Open Distribution System Simulator (OpenDSS) software. Case studies have confirmed the potency of the developed multilevel approach for the close coordination of VVC devices, and non-generation resources, such as demand response and energy storage to lower the losses and maintain a system-wide voltage profile.**

Index Terms—**Day-Ahead Pricing, Demand Response, energy Storage, On-load Tap Changer, Voltage Regulation, Wind Generation.**

I. Introduction

THE tendency to move to a dense wind generations (WGs) integrated on the distribution system, have unequivocal benefits in terms of sustainable energy development [1], [2]. The variable and fluctuating nature of WGs can eventually sprawl to undermine network's reliability [3]. The limited dispatchability of wind generation dispersed in large proportions, could cause grid voltage rise or voltage dip during low WGs [4]. It can also disrupted operation of voltage control devices [5]. At the distribution substation, an on-load tap changing transformer (OLTC) is generally used to control the secondary bus voltage of the main transformer [6].

Shunt capacitors are usually used in feeder system to provide reactive power compensation, so as to keep the voltage profile within the permissible limits [7]. Conventional voltage regulator devices may not be sufficient to solve voltage variation challenges. This is especially true in distribution system with a high R/X ratio, where the massive injection of active power from wind energy can exacerbate the issue.

Energy storage (ES) is a deployable asset that has multifaceted benefits including variety of applications to deal with the variability of WGs at a large scale [8]. In particular, ES can address issues concerning voltage support and load following [9], [10]. Demand response (DR) is the modification of end-user consumer consumption habits in response to changes in energy prices over time or incentive payments made by the utility provider [11]. Load curtailments through DR can also provide further leverage on feeder circuit voltage profile [12]. Both of ES and DR are indispensable non-generation supporting technologies in distribution network [13].

Scheduling of the OLTC and shunt capacitors can also maintain acceptable distortion levels, when taking harmonics into consideration [14]. The use of the OLTC to mitigate the voltage increase brought on by the connection of numerous wind generations to the medium-voltage (MV)/low-voltage (LV) distribution system was addressed in [15]. The centralized coordination between the conventional voltage/VAr control (VVC) devices was carried out for optimal voltage regulation in a distribution system with PV generation [16], [17] using genetic algorithms (GAs) [18].

The proper size and strategic sitting of the ES can provide grid operational support to facilitate the coordinated operation of components in the system [19]. The coordinated control strategy for distribution network was reviewed in [20], [21] and carried out in [22]. To solve the ideal location and capacity for ES units, a hybrid multiobjective particle swarm optimization method was taken into consideration [23]. Demand response was applied to keep distribution feeder voltages within specified ranges [12], [13]. Although the OLTC and the DR were coordinated, the problem was not constructed as an optimization problem. The combined effect of the network reconfiguration, DR, and optimum size and location of WGs were studied using particle swarm optimization (PSO) with

Manuscript received March 13, 2025; revised June 20, 2025.

J. O. Petinrin is a Chief Lecturer at the Department of Electrical and Electronic Engineering, Federal Polytechnic Ede, Ede, Nigeria (e-mail: jopetinrin2@gmail.com).

O. O. Petinrin is a Lecturer at the Department of Electrical and Electronic Engineering, Federal Polytechnic Ede, Ede, Nigeria (e-mail: petinrin.oluyemi@federalpolyede.edu.ng).

M. O. Petinrin is a Reader at the Department of Mechanical Engineering, University of Ibadan, Ibadan, Nigeria (corresponding author e-mail: layopet01@yahoo.com).

I. I. Ogedengbe is a Lecturer at the Department of Mechanical Engineering, Federal University of Technology, Akure, Nigeria (e-mail: iiogedengbe@futa.edu.ng).

constriction factor [24].

The paper proposes a mathematical programming framework to reduce voltage stochastic variable and energy losses subject to system operating conditions and equipment limits, for the next-day operation schedule. The collaborative non-generation resources of ES assets and DR options, to provide other levels of voltage regulation. Contrary to snapshot analysis, which does not account for the progression of time, quasi-static time series simulation is considered to analyze the interaction between WGs, VVC devices, ES and DR chronologically. Particle swarm optimization with gravitational search algorithm (PSOGSA), which is used for ES and DR, is used to solve the resulting mixed-integer mathematical programming problem. over a multiperiod time simulation of 24 hours while VAr control devices are not optimized but operated as explained in section iv.

II. Proposed Voltage Control Framework

The conventional objective of distribution [25] system VVC is to find out the optimal dispatch of the VVC devices for the next 24 hours. More specifically, the OLTC tap positions including feeder SVRs, and on/off status of shunt capacitors at each hour need to be determined, such that feeder node voltage variations can be restrained, and total network losses are minimized. Thus, the distribution system's active power losses and feeder node voltage deviation can be used to formulate the objective function.:

$$\text{Min } F = w_v \sum_{i=1}^{N}\sum_{t=1}^{24}\left\|V_{i,t} - V_i^{ref}\right\|^2 + w_l \sum_{i=1}^{N}\sum_{t=1}^{24} P_{Li,t}\ \Delta t \quad (1)$$

The entire power losses, including energy storage, are calculated as follows (Dopazo et al., 1967):

$$P_L = \sum_{i}^{N}\sum_{j}^{N}\begin{bmatrix}\alpha_{ij}\left(P_iP_j + Q_iQ_j\right) \\ +\beta_{ij}\left(P_iQ_j - Q_{i,t}P_j\right)\end{bmatrix} \quad (2)$$

where,

$$\alpha_{ij} = \frac{r_{ij}}{V_iV_j}\cos\left(\delta_i - \delta_j\right)$$

$$\beta_{ij} = -\frac{r_{ij}}{V_iV_j}\sin\left(\delta_i - \delta_j\right)$$

$Z_{ij} = r_{ij} + x_{ij}$ is the *ij*th element of [*Zbus*] bus impedance matrix

$$P_{i,t} = P_{WGi,t} - P_{Di,t} \pm P_{ESi,t}$$

$$Q_{i,t} = Q_{WGi,t} - Q_{Di,t} \pm Q_{ESi,t}$$

The subscript *t* indicates a particular time or hour of the day. Power flow equality constraints, which are among the restrictions, include:

$$P_{i,t} = V_{i,t} \times \sum_{j=1}^{N} V_{j,t}\left[G_{i,j}\cos\left(\delta_{i,t} - \delta_{j,t}\right) + B_{i,j}\sin\left(\delta_{i,t} - \delta_{j,t}\right)\right] \quad (3)$$

$$Q_{i,t} = V_{i,t} \times \sum_{j=1}^{N} V_{j,t}\left[G_{i,j}\sin\left(\delta_{i,t} - \delta_{j,t}\right) - B_{i,j}\cos\left(\delta_{i,t} - \delta_{j,t}\right)\right] \quad (4)$$

$$V_{\min,t} \le V_{i,t} \le V_{\max,t} \qquad i \in N \quad (5)$$

where (5) is for voltage upper and lower limits.

A. Voltage/var Control (VVC) Devices

The OLTC mechanisms usually affect the secondary bus voltage of the substation's main transformer as well as the local step voltage regulators (SVRs) connected to primary feeders [26], [27]. the OLTCs' maximum permitted switching operations are:

$$\sum_{t=1}^{24}\left|TAP_t - TAP_{t-1}\right| \le K_{TAP} \quad (6)$$

$$TAP_{\min,t} \le TAP_t \le TAP_{\max,t} \quad (7)$$

$$\left[V_s\right]_{abc,t} = \left[n_R\right]_{abc,t}\left[V_R\right]_{abc,t} \quad (8)$$

$$n_R = 1 \pm TAP_t \cdot \Delta V_{TAP} \quad (9)$$

where ΔV_{TAP} the tap change step. Maximum switching operations of shunt capacitors, as well as capacitor limits are:

$$\sum_{t=1}^{24}\left(C_{c,t} \oplus C_{c,t-1}\right) \le K_c;\ c = 1,2,....,nc \quad (10)$$

$$Q_{c(i,t)} = B_c V_{(i,t)}^2, c = i \quad (11)$$

$$Q_{c,\min} \le Q_{c,i} = Q_{c,\max} \quad (12)$$

The above equations implicitly account for the OLTC bandwidth and time delay as well as the capacitor control. The OLTC moves first with a time delay of 15 seconds, while the time delay between the OLTC and SVR is 30 seconds. The criterion is set, in the subsequent case studies, such that the shunt capacitor is to switch 'on' when the reactive power flow in the line is 50% of the capacitance magnitude. It is directed at downstream loads and switches 'off' when reverse reactive power flow is 75% the size of the capacitor.

B. Energy Storage

Grid-level energy storage provides a flexible and rapid response resource that can counterpoise the WGs intermittency and smooth their energy output over time.

The exact loss formula is used to represent the total real power loss as in WGs. Technical constraints of the ES, which were included subtly in (2) and (3), can be expressed in more detail in the context of net active power injection as follows:

$$P_{i,t} = P_{WG_{i,t}} - P_{D_{i,t}} \pm P_{ES_{m,t}}\ i = m,\ m \in M, M \subseteq N \quad (13)$$

Computational Procedure for Optimal Sizing and Sitting of Energy Storage

An optimal capacity and location of ES can facilitate power quality management, peak energy demand fulfilment, reduce distribution network expansion costs, increase the advantages of WG integration and DERs [28].

Since the Wind turbines used in this study is of unity power factor, the ES also is of unity power factor (i.e. θ = 1, 'k' = zero). More so, it is not economically worthwhile for ES to inject reactive power; a capacitor is a better option. For the least amount of energy loss, the ideal size of ES at each bus i is given by (14) [29], [30].

$$P_{ESi,t} = P_{Di,t} - \frac{1}{\alpha_{ii}}\left[\sum_{j=1,\, j\neq i}^{N}\left(\alpha_{ij}P_j - \beta_{ij}Q_j\right)\right] \qquad (14)$$

At the nth load level, the energy loss of the distribution grid before compensation can be expressed as:

$$E_{Loss,n} = T_n P_{Loss,n} \qquad (15)$$

The energy loss after compensation is expressed as:

$$E_{Loss,n} = T_n P^{C}_{Loss,n} \qquad (16)$$

where T_n is the time duration at the nth load level, $P_{Loss,n}$ is the power loss at the nth load level before compensation and $P^{C}_{Loss,n}$ is the power loss at the nth load level after compensation.

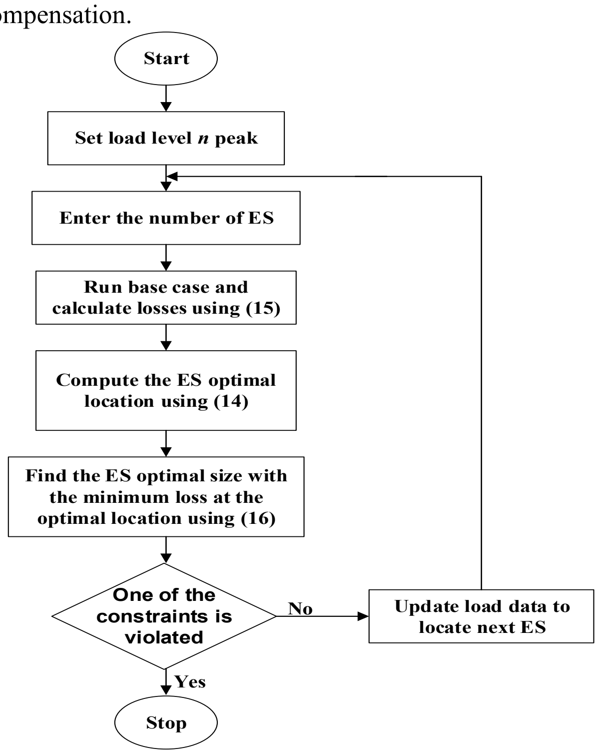

Figure 1. Flow chart of energy storage sizing and siting computational procedure.

The application of analytical techniques to compute optimal placements assists to decrease the solution space. The optimal placement is found after one power flow run. The flow chart of the computational procedure is depicted in Figure 1 and is elucidated below:

(i) Run the base case power flow and find energy loss using (15).

(ii) Find the optimal ES location as follows:

Compute the optimal size of ES at each node using (14), unavailability of the maximum number of ES; new iteration loss is higher than the former iteration loss; the former iteration loss is maintained.

C. Demand Response

Energy storage is a technology that has historically been employed for arbitrage, where surplus low-cost energy was held during off-peak hours, such as the evenings and weekends, and then released back into the grid during more expensive peak times. However, ES is not a cost-competitive option at large-scale integration levels of renewable energy [31]. Therefore, non-storage options, which can provide for lower cost mitigation, can be effective.

Demand response (DR) is a potentially cost-effective alternative approach that can manage the variability nature of wind energy. With the expected proliferation of smart metering infrastructure (AMI) in retail households, real Time Pricing (RTP) can offer substantial cost savings for utilities, as well as maintain the efficiency of electricity markets [11].

Presumably, customers are equipped with smart meters that enable them to respond to a proper price signal and communicate through a ubiquitous bidirectional communication infrastructure with load-serving entities (LSEs). Therefore, customers can receive real-time prices from the real-time spot energy market or hourly price information for the next day from the day-ahead energy market.

The aggregators submit bids specifying the amount of curtailment and the duration of the day-ahead energy market. If the bids are accepted, a non-compliance penalty is imposed [32].

The load demand (P_D) can be categorized into elastic and inelastic loads, given as:

$$P_{D_{r,t}} = P_{U_{r,t}} + P_{E_{r,t}} \qquad r \in R_j \quad j = 1,2,...,D \qquad (17)$$

Elastic loads (P_E) can be further divided into controllable and time-shiftable loads. Thermostatically regulated loads such as heating, air-conditioning (HVAC) and ventilation loads are controllable loads (P_C). While time-shiftable loads (P_S), which include electric cars, washing machines, etc., are loads that can be moved to a different time. Lighting loads are examples of inelastic loads (P_U), which are loads that cannot be moved or regulated. Thus;

$$P_{E_{r,t}} = P_{C_{r,t}} + P_{S_{r,t}} \qquad r \in R_j \quad j = 1,2,...,D \qquad (18)$$

Suppose a customer r switches a set of A_r equipment. For each equipment $a \in A_r$, at time t, the power taken is shown by the symbol $P_{ra,t}$. P_{ra} represents the total energy consumed by appliance a of customer r for the whole day.

$$P_{C_{r,t}} = \sum_{a} P_{ra,t} \quad \forall a \in A_r \qquad (19)$$

$$P_{S_{r,t}} = \sum_{a}\sum_{t'} P_{S_{a,t't}} - \sum_{a}\sum_{t'} P_{S_{a,tt'}}$$
$$\forall t,t' \in T := \{1,2,\ldots,24\} \qquad (20)$$

$$0 \leq \sum_{j}^{D}\sum_{r}^{R_j}\sum_{a}^{A_r} P_{S_{ra,tt'}} \leq \sum_{j}^{D}\sum_{r}^{R_j}\sum_{a}^{A_r} R_j^{+} \times P_{ra,t}$$
$$R_j^{+} := \max\{r\} \qquad (21)$$

$$P_{S_{a,tt''}} = 0 \quad \forall t, t'' \in T,\ \forall a \in A_r \tag{22}$$

Equation (19) describes available controllable load at time t, whereas (20) expresses the net load shifted to time t. Equation (21) caps the total shifted load from time t to time t' to be less than or equal to the actual loading of all appliances at time t. Equation (22) makes sure that the operating time of the relocated load is not moved to an earlier time.

D. The decision taken by end-use customers, through their aggregators, is purely based on economic aspects to maximize their social welfare. Hence;

$$\bar{\lambda}\sum_{t=1}^{24} P_{U_{r,t}} + \sum_{t=1}^{24}\hat{\lambda}_t P_{E_{r,t}} \le \bar{\lambda}\sum_{t=1}^{24}\left[P_{U_{r,t}} + P_{E_{r,t}}\right] \quad r \in R_j \tag{23}$$

$$\hat{\lambda}_t \le \bar{\lambda} \quad \forall t \in T \tag{24}$$

Constraint (23) should provide the right incentive to participate in the DR plan. Its aim is to make sure the payments of elastic customers is less than non-elastic ones. Equation (24) ensures that the DAP is less than the flat price, albeit this may not be always the case in practice.

Demand response strategies are intrinsically economic tools that enable customer participation in wholesale energy markets, through equity pricing, to increase system reliability and improve market liquidity. The novelty refers to in (23) is that it simply integrates economic facets of the DR seamlessly into a comprehensive near-traditional technical framework for voltage control.

To ascertain that DR works properly to minimize system losses, we have

$$P_{Li,t}^{with\ DR} \le P_{Li,t}^{without\ DR} \tag{25}$$

Equations (1) to (25) provide a comprehensive mathematical programming description for the voltage control problem, encompassing the model of ES and DR choices required to reduce the impact of renewable energy's fluctuating voltage profile and system losses.

III. Overall Methodology

The switching operation of shunt capacitors, an integer problem, brings extra difficulties to a nonlinear optimization problem. Stochastic meta-heuristics such as particle swarm optimization (PSO) is a good numerical method to search for an approximate global optimal solution for these kinds of problems. Moreover, PSO can handle mixed-integer nonlinear optimization problems efficiently [33].

This paper employs a hybrid PSOGSA, a combination of PSO and a gravitational search algorithm (GSA), to solve the resulting voltage control issue. The heterogeneous combination (using one after the other) of the functionality of

PSO and GSA extend the strengths of both techniques in exploration and exploitation. The hybrid PSOGSA method is outlined in [17].

The fitness function used in this paper is given as:

$$\text{Fitness} = -\left[w_v\sum_{i=1}^{N}\sum_{t=1}^{24}\left\|V_{i,t} - V_i^{ref}\right\|^2 + w_l\sum_{i=1}^{N}\sum_{t=1}^{24}P_{Li,t}\right] \tag{26}$$

IV. Case Studies

IEEE 123 bus-modified test feeder of a real 115 kV/4.16 kV, 50-Hz distribution system is utilized to evaluate the proposed multi-layer voltage control scheme. The overall load is adjusted to 16 MW, and the energy users are split between businesses and homes. The modified IEEE 123 test feeder consists of an overhead line with multiple feeder regulators in series along the three-phase primary line. It also consists of a normally open switch and a normally closed switch. The

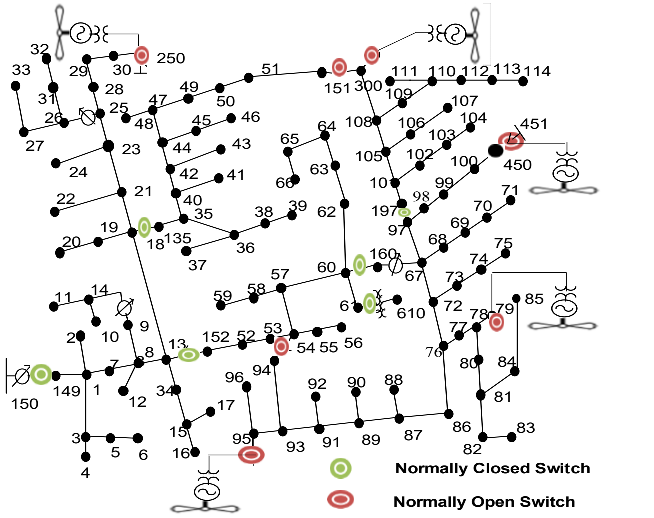

Figure. 3. IEEE 123 bus modified test feeder.

normally closed switch is always in a closed position except for the maintenance of the line at which it is connected. The normally open switch is incorporated to connect the wind energy when necessary [34]. The test feeder is depicted in Figure 3, consists of four SVRs and an OLTC transformer.

Weighting factors are scalar coefficients that are multiplied by each variable are as follows:

$$\sum_{k=1}^{K} W_k = 1 \tag{27}$$

Therefore, $w_v + w_l = 1$.

The weighting factors are designated as $w_v = 0.55$ and $w_l = 0.45$ for voltage deviations and energy losses respectively, following various simulations.

(a). Coordination of VVC Devices, ES, and DR for voltage regulation

The updated 16 MW peak demand network includes a 30% (4.8 MW) wind production. The appropriate system real energy losses and voltage profile are produced using the optimal configurations of the VVC devices, including the ES/DR, shunt capacitors (SCs) and the load tap changers (LTCs), and was achieved in OpenDSS with the COM interface in MATLAB. The stated objectives of the study are accomplished by synchronizing the ES and DR with LTCs for effective operation. The results of a 24-hour quasi-static time series simulation of the system are shown in Figure 4. It has been noted that the LTCs were unable to keep the voltage within permitted ranges. The voltage pattern remains less of the voltage limitations for several hours during the day after turning on the SCs. capacitors significantly improve reactive power flow, reducing line current and voltage drop. Losses are decreased and the voltage profile is improved when more and more capacitor banks are used.

Considering that the maximum charging and discharging rates are each six hours, the battery storage is split into two portions. To prevent the battery from being entirely exhausted before it is recharged, the setting for the charging trigger is 100%, while the setting for the discharging trigger is 90%. Figure 5 shows the charging, discharging, and idle hours for each segment. The ES and VVC devices are coordinated together. The ES's dispatch function adds extra power to the feeder. It is clear from Figure 4 that the ES integration has rendered an improvement in the voltage profile as well as a decrease in energy loss. The voltage was completely restored to be within the statutory limits (± 5%). The ES is turned off to level the feeder's peak valley, and the DR is implemented through the DAP at the four zones. DR is now coordinated alone with the VVC devices. The result is shown in Figure 4. It appears the DR has a more robust impact on the system voltage as compared. DR has not only improved the overall system voltage but also managed to flatten the voltage profile in general. The energy losses at the eleventh hour of the day are detailed in row 7 and 8 in Table 1, along with the corresponding percentage loss reduction. The updated 16 MW peak demand network which includes a 30% (4.8 MW) wind energy was replaced with solar energy of the same capacity in order to compare the effectiveness of the control devices. The appropriate system real energy losses and voltage profile are produced using the optimal configurations of the same control devices. The energy losses at the eleventh hour of the day with the solar energy are depicted in the last two rows in Table 1, along with the corresponding percentage loss reduction. The insignificant differences shows the effectiveness of the control devices.

The implementation of ES and DR appears to reduce the loss of energy and increase the percentage of loss reduction. Voltage is raised as a result of the reduction in energy loss. When the ES is distributed and the DR is put into place, peak load demand is reduced, and controllable load is adjusted to changing wind generation.

Figure 6 illustrates the tap operation of the LTC at various times of the day. Without any additional controls, the LTC tap only moves once. However, even moving to the highest position of 16, it was unable to raise the voltage to the required level. When the SCs are turned "on," the tap position changes with 5 operations from 8 to 10. The tap now operates four times with a tap position ranging from one to three due to the integration of the ES. To maintain the voltage within the allowable voltage limits, the tap position advances three times when the DR is applied, from a position between -1 and 2. This demonstrates that using the ES or the DR as contrasted to just VVC devices relieves the load on the LTCs.

The voltage is brought back to the permissible limits by coordinating the VVC devices with either ES or DR even though the LTC tap moves three times in a 24-hour period with the smallest tap position. In this test example, the results have repeatedly shown that the system losses are decreased and the system's ability to maintain the system voltages is improved due to the coordination of the VVC devices with ES and DR.

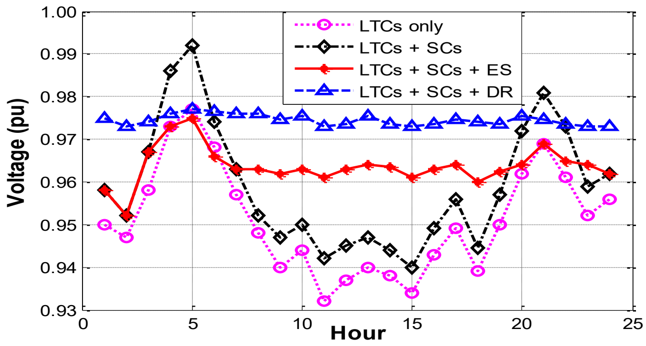

Figure 4 Introduction of control devices at various levels.

TABLE 1

VOLTAGE PROFILE LTCS AND LOSSES WITH AND WITHOUT ES AND DR

	LTCs	SCs	ES	DR
Minimum Voltage (pu)	0.9314	0.9406	0.9519	0.9733
Maximum Voltage (pu)	0.9769	0.9919	0.9760	0.9772
No. of Tap	1	5	4	3
Voltage Deviation	0.0455	0.0513	0.0241	0.0039
Tap position	16	8 to 10	1 to 3	-1 to 2
Losses (kW) with Wind	1780.59	1310.40	1170.40	928.01
Loss Reduction (%) with wind	-	26.41	34.27	47.88
Losses (kW) with solar	1780.47	1310.43	1170.44	928.38
Loss Reduction (%) with solar	-	26.40	34.26	47.86

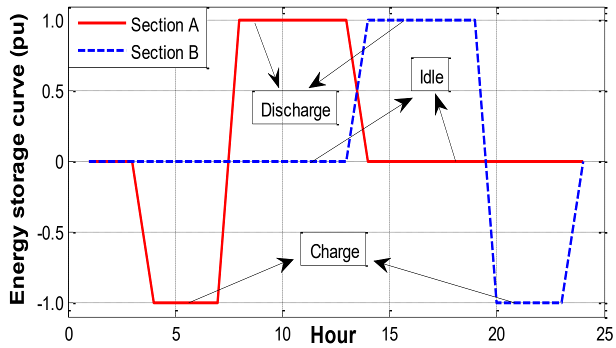

Figure 5. Energy storage dispatch curve.

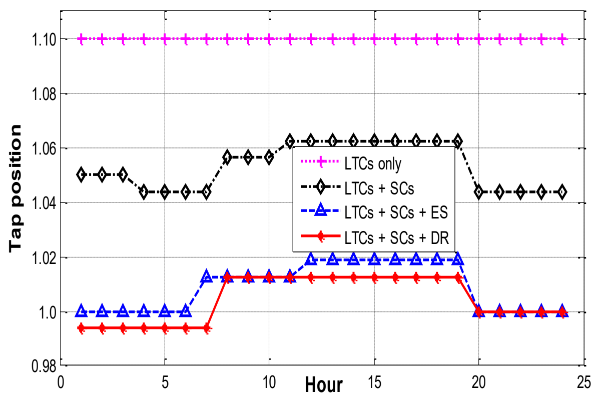

Fig. 6. Regulator tap position at various levels.

Distribution of ESs successfully aids in the integration of variable wind energy sources, lowers energy losses, and enhances the voltage profile. The application of DR highlights its ability to address the voltage depression issue in a distribution grid when other control devices' coordination was insufficient raise the voltage. Additionally, it gives the system more flexibility to protect against variations in wind energy.

(b). Demand response option for load leveling

Load leveling or shifting load from the peak hour to the off-peak hour, is beneficial for reducing fluctuations in energy demand during the day, which can eventually lead to the deferral of capacity upgrades. The application of the demand response (DR) for a heavy integration level of wind energy in the feeder for one week is investigated in this scenario. At a 16 MW peak load, the feeder load stays constant. However, the feeder now comprises a weekly power usage curve. Chronological 1-week (168-hour) simulation of the system is done, and results are displayed in Fig. 7 and Fig. 8. Application of the DR turned out to be inapt to recover the voltage within acceptable bounds on the third day due to substantial drop in wind production; as a result of low wind speed. Therefore, ES is called in to supply more power to the feeder to prop the voltage to be higher than the permissible lower bound of 0.95 pu. The load MW, wind power and net load power encompassing demand response and energy storage are depicted in Fig. 8. It is apparent, from Fig. 8, that the use of the DR and the ES have flattened the net residual load profile and shaved fluctuations to almost a constant value of 8 MW. Results in Fig. 8, assert the viability of the DR in addressing the load leveling strategy in the operation timescale. On the other hand, this case study demonstrates that the created framework is not only useful and efficient for controlling voltage over a 24-hour period, but also for controlling voltage over longer time periods that account for a sudden decrease in wind generation.

The base case losses of the system are 1.031 MW. However, system losses drop, with the wind penetration considered, to 0.786 MW and 0.598 MW when the DR is applied respectively. This indicates that the distribution system losses have experienced a reduction of 24% with the integration of wind generation only. It increases to a staggeringly 42%, when the DR is applied along with local wind generation. The impact of load leveling on loss reduction and voltage profile improvement on distribution system is less acknowledged in the literature [35].

In this case, DR was engaged first since it is a cheaper option. Furthermore, as the DR could not restore the system voltage per sec independently. Therefore, ES is tapped when needed only at the third day since it is a pricy option after all. This is a viable modus operandi to minimize operation costs that has a paramount importance in utility practices. Such an issue is subtly included in this paper, assumingly through the locations and sizes of the ES procured by the DNO. This test case also shows that at times, DR may not be the silver bullet that can solve all distribution network problems. ES still can be instrumental to maintain a near-constant load profile.

This, once again, underlines the adequacy of the developed multilevel framework to handle wide scope of operating conditions and test scenarios. It also highlights that Es and DR are not competing technologies, but rather they work in tandem with variable wind generation to maintain smart, reliable and efficient operation of the grid.

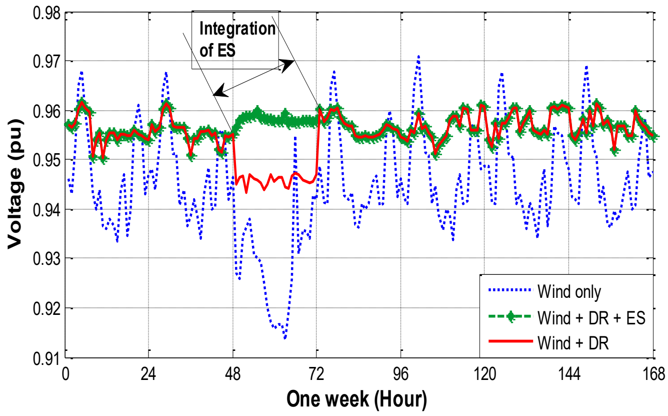

Fig. 7. Voltage profile of the application of DR and ES to load leveling for one month.

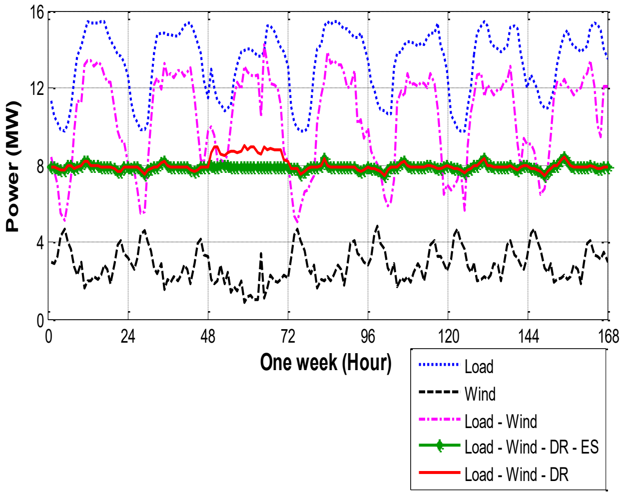

Fig. 8. Net load demand for one week.

Conclusion

High penetration of wind energies has created a number of collateral impacts on the distribution system. Voltage rise comes at the forefront of these impacts. This study has demonstrated a multilevel sequential optimization framework that consists of voltage/VAr control (VVC) devices, coupled with the ES and DR, at different stages if necessary. The prime objective is to mitigate voltage variations, reduce system losses, and offset the intermittency resulting from wind energy units connected to the distribution system. The unique DR modeling devised herein seamlessly integrate economic aspects of the DR into an extensive technical framework for voltage control. Applying the developed multilevel approach to the IEEE 123 bus test feeder over many test cases and operating scenarios, has highlighted its competency in providing equitable dispatch, by complementing the use of several control alternatives, and ameliorating the overall system performance. The framework also has the capability to do energy scheduling for a single day or multiple days ahead.

Unlike snapshot analysis, which does not account for the worth of time, a main attribute of variable generation, the multiperiod time series simulation approach, adopted in this paper, is capable of analyzing the interaction between wind energy, VVC devices, ES and DR and capturing the time-dependency nature between them in an hourly operation timescale.

REFERENCES

[1] Z. Li and F. Liu, “Frequency and voltage regulation control strategy of Wind Turbine based on supercapacitors under power grid fault,” *Energy Reports*, vol. 10, pp. 2612–2622, Nov. 2023, doi: 10.1016/J.EGYR.2023.09.067.

[2] E. I. Come Zebra, H. J. van der Windt, G. Nhumaio, and A. P. C. Faaij, “A review of hybrid renewable energy systems in mini-grids for off-grid electrification in developing countries,” *Renewable and Sustainable Energy Reviews*, vol. 144, p. 111036, Jul. 2021, doi: 10.1016/J.RSER.2021.111036.

[3] W. Wangdee and R. Billinton, “Probing the intermittent energy resource contributions from generation adequacy and security perspectives,” *IEEE Transactions on Power Systems*, vol. 27, no. 4, pp. 2306–2313, 2012, doi: 10.1109/TPWRS.2012.2204281.

[4] N. Mansouri, A. Lashab, J. M. Guerrero, and A. Cherif, “Photovoltaic power plants in electrical distribution networks: a review on their impact and solutions,” *IET Renewable Power Generation*, vol. 14, no. 12, pp. 2114–2125, Sep. 2020, doi: 10.1049/IET-RPG.2019.1172.

[5] A. Baviskar, K. Das, M. Koivisto, and A. D. Hansen, “Multi-Voltage Level Active Distribution Network with Large Share of Weather-Dependent Generation,” *IEEE Transactions on Power Systems*, vol. 37, no. 6, pp. 4874–4884, Nov. 2022, doi: 10.1109/TPWRS.2022.3154613.

[6] S. R. Shukla, S. Paudyal, and M. R. Almassalkhi, “Efficient Distribution System Optimal Power Flow With Discrete Control of Load Tap Changers,” *IEEE Transactions on Power Systems*, vol. 34, no. 4, pp. 2970–2979, Jul. 2019, doi: 10.1109/TPWRS.2019.2894674.

[7] Z. Tang, D. J. Hill, and T. Liu, “Distributed Coordinated Reactive Power Control for Voltage Regulation in Distribution Networks,” *IEEE Trans Smart Grid*, vol. 12, no. 1, pp. 312–323, Jan. 2021, doi: 10.1109/TSG.2020.3018633.

[8] J. O. Petinrin and M. Shaabanb, “Impact of renewable generation on voltage control in distribution systems,” *Renewable and Sustainable Energy Reviews*, vol. 65, pp. 770–783, Nov. 2016, doi: 10.1016/J.RSER.2016.06.073.

[9] S. Hou and T. Murata, “Multi-objective Demand Responding Micro Grid Dispatch Optimization based on Energy Storage Operation with Uncertain RES Power,” in *Lecture Notes in Engineering and Computer Science: Proceedings of The International Multi Conference of Engineers and Computer Scientists, October 20-22, 2021*, 2021, pp. 1–6.

[10] D. Stenclik, P. Denholm, and B. Chalamala, “Maintaining Balance: The Increasing Role of Energy Storage for Renewable Integration,” *IEEE Power and Energy Magazine*, vol. 15, no. 6, pp. 31–39, Nov. 2017, doi: 10.1109/MPE.2017.2729098.

[11] F. Shariatzadeh, P. Mandal, and A. K. Srivastava, “Demand response for sustainable energy systems: A review, application and implementation strategy,” *Renewable and Sustainable Energy Reviews*, vol. 45, pp. 343–350, May 2015, doi: 10.1016/J.RSER.2015.01.062.

[12] A. Zakariazadeh, O. Homaee, S. Jadid, and P. Siano, “A new approach for real time voltage control using demand response in an automated distribution system,” *Appl Energy*, vol. 117, pp. 157–166, Mar. 2014, doi: 10.1016/J.APENERGY.2013.12.004.

[13] B. Kroposki; A. Bernstein; J. King; D. Vaidhynathan; X. Zhou; C. Chang, “Autonomous Energy Grids: Controlling the Future Grid with Large Amounts of Distributed Energy Resources,” *IEEE Power and Energy Magazine*, vol. 18, no. 6, pp. 37–46, Nov. 2020, doi: 10.1109/MPE.2020.3014540.

[14] M. J. Milovanović and J. N. Radosavljević, “A Hybrid PPSOGSA Algorithm for Optimal Volt/VAr/THDv Control in Distorted Radial Distribution Systems,” *Applied Artificial Intelligence*, vol. 35, no. 3, pp. 227–246, Feb. 2021, doi: 10.1080/08839514.2020.1855380.

[15] E. O. Hasan, A. Y. Hatata, E. A. Badran, and F. M. H. Yossef, “Optimal coordination of voltage control devices in distribution systems connected to distributed generations,” *Electrical Engineering*, vol. 101, no. 1, pp. 175–187, Apr. 2019, doi: 10.1007/S00202-019-00764-2/METRICS.

[16] N. Mahmud and A. Zahedi, “Review of control strategies for voltage regulation of the smart distribution network with high penetration of renewable distributed generation,” *Renewable and Sustainable Energy Reviews*, vol. 64, pp. 582–595, Oct. 2016, doi: 10.1016/J.RSER.2016.06.030.

[17] X. Zhang, Z. Wang, and Z. Lu, “Multi-objective load dispatch for microgrid with electric vehicles using modified gravitational search and particle swarm optimization algorithm,” *Appl Energy*, vol. 306, p. 118018, Jan. 2022, doi: 10.1016/J.APENERGY.2021.118018.

[18] T. Senjyu, Y. Miyazato, A. Yona, N. Urasaki, and T. Funabashi, “Optimal distribution voltage control and coordination with distributed generation,” *IEEE Transactions on Power Delivery*, vol. 23, no. 2, pp. 1236–1242, Apr. 2008, doi: 10.1109/TPWRD.2007.908816.

[19] A. Askarzadeh, “Capacitor placement in distribution systems for power loss reduction and voltage improvement: a new methodology,” *IET Generation, Transmission & Distribution*, vol. 10, no. 14, pp. 3631–3638, Nov. 2016, doi: 10.1049/IET-GTD.2016.0419.

[20] N. Hashemipour, Aghaei j., Lotfi M., and Niknam T., “Multi-objective optimisation method for coordinating battery storage systems, photovoltaic inverters and tap changers,” *IET Renewable Power Generation*, vol. 14, no. 3, pp. 475–483, Feb. 2020, doi: 10.1049/IET-RPG.2019.0644.

[21] X. Liu, A. Aichhorn, L. Liu, and H. Li, “Coordinated control of distributed energy storage system with tap changer transformers for voltage rise mitigation under high photovoltaic penetration,” *IEEE Trans Smart Grid*, vol. 3, no. 2, pp. 897–906, 2012, doi: 10.1109/TSG.2011.2177501.

[22] Z. Lei, Q. Xu, G. Hao, C. Wei, and M. Yang, “Voltage Coordination Control Strategy for Low Voltage Distribution Networks in Western Rural Areas under Photovoltaic Storage Access.,” *Engineering Letters*, vol. 32, no. 7, pp. 1412–1423, 2024.

[23] S. Wen, H. Lan, Q. Fu, D. C. Yu, and L. Zhang, “Economic allocation for energy storage system considering wind power distribution,” *IEEE Transactions on Power Systems*, vol. 30, no. 2, pp. 644–652, Mar. 2015, doi: 10.1109/TPWRS.2014.2337936.

[24] K. D. Mistry and R. Roy, “Impact of demand response program in wind integrated distribution network,” *Electric Power Systems Research*, vol. 108, pp. 269–281, Mar. 2014, doi: 10.1016/J.EPSR.2013.11.018.

[25] P. Srivastava, R. Haider, V. J. Nair, V. Venkataramanan, A. M. Annaswamy, and A. K. Srivastava, “Voltage regulation in distribution grids: A survey,” *Annu Rev Control*, vol. 55, pp. 165–181, Jan. 2023, doi: 10.1016/J.ARCONTROL.2023.03.008.

[26] K. Gholami, M. R. Islam, M. M. Rahman, A. Azizivahed, and A. Fekih, “State-of-the-art technologies for volt-var control to support the penetration of renewable energy into the smart distribution grids,” *Energy Reports*, vol. 8, pp. 8630–8651, Nov. 2022, doi: 10.1016/J.EGYR.2022.06.080.

[27] X. Cai, Z. Yang, P. Liu, X. Lian, Z. Li, G. Zhu, and H. Geng, “Voltage Control Strategy for Large-Scale Wind Farm with Rapid Wind Speed Fluctuation,” *Energies 2024, Vol. 17, Page 2220*, vol. 17, no. 9, p. 2220, May 2024, doi: 10.3390/EN17092220.

[28] C. K. Das, O. Bass, G. Kothapalli, T. S. Mahmoud, and D. Habibi, “Overview of energy storage systems in distribution networks: Placement, sizing, operation, and power quality,” *Renewable and Sustainable Energy Reviews*, vol. 91, pp. 1205–1230, Aug. 2018, doi: 10.1016/J.RSER.2018.03.068.

[29] M. Shaaban and J. O. Petinrin, “Integration of Energy Storage for Voltage Support in Distribution Systems with PV Generation,” *J Electr Eng Technol*, vol. 11, no. 5, pp. 1077–1083, 2016, doi: 10.5370/JEET.2016.11.5.1077.

[30] J. O. Petinrin and M. Shaaban, “Multiperiod Coordination of Local Voltage Controllers and Energy Storage for Voltage Regulation in Distribution Feeder-Connected Renewable Energy Sources,” *Iranian Journal of Science and Technology - Transactions of Electrical Engineering*, vol. 43, no. 3, pp. 531–544, Sep. 2019, doi: 10.1007/S40998-018-0092-2/METRICS.

[31] M. Esteban, Q. Zhang, and A. Utama, “Estimation of the energy storage requirement of a future 100% renewable energy system in Japan,” *Energy Policy*, vol. 47, pp. 22–31, Aug. 2012, doi: 10.1016/J.ENPOL.2012.03.078.

[32] R. Walawalkar, S. Fernands, N. Thakur, and K. R. Chevva, “Evolution and current status of demand response (DR) in electricity markets: Insights from PJM and NYISO,” *Energy*, vol. 35, no. 4, pp. 1553–1560, Apr. 2010, doi: 10.1016/J.ENERGY.2009.09.017.

[33] K. Y. Lee and M. A. El-Sharkawi, “Modern Heuristic Optimization Techniques: Theory and Applications to Power Systems,” *Modern Heuristic Optimization Techniques: Theory and Applications to Power Systems*, pp. 1–586, Jun. 2007, doi: 10.1002/9780470225868.

[34] K. P. Schneider *et al.*, “Analytic Considerations and Design Basis for the IEEE Distribution Test Feeders,” *IEEE Transactions on Power*

Systems, vol. 33, no. 3, pp. 3181–3188, May 2018, doi: 10.1109/TPWRS.2017.2760011.

[35] S. A. Adegoke, Y. Sun, A. S. Adegoke, and D. Ojeniyi, "Optimal placement of distributed generation to minimize power loss and improve voltage stability," *Heliyon*, vol. 10, no. 21, p. e39298, Nov. 2024, doi: 10.1016/J.HELIYON.2024.E39298.